

IAC-12-B4.7B.3

TANDEM-X: A RADAR INTERFEROMETER WITH TWO FORMATION FLYING SATELLITES

Gerhard Krieger, Manfred Zink, Alberto Moreira

Microwaves and Radar Institute
German Aerospace Center (DLR)
Oberpfaffenhofen, Germany
gerhard.krieger@dlr.de

TanDEM-X (TerraSAR-X add-on for Digital Elevation Measurements) is an innovative formation flying radar mission that opens a new era in spaceborne radar remote sensing. The primary objective is the acquisition of a global Digital Elevation Model (DEM) with unprecedented accuracy (12 m horizontal and 2 m vertical resolution). This goal is achieved by extending the TerraSAR-X synthetic aperture radar (SAR) mission by a second, TerraSAR-X like satellite (TDX) flying in close formation with TerraSAR-X (TSX). Both satellites form together a large single-pass SAR interferometer with the opportunity for flexible baseline selection. This enables the acquisition of highly accurate cross-track interferograms without the inherent accuracy limitations imposed by repeat-pass interferometry due to temporal decorrelation and atmospheric disturbances. Besides the primary goal of the mission, several secondary mission objectives based on along-track interferometry as well as new bistatic and multistatic SAR techniques have been defined, representing an important and innovative asset of the TanDEM-X mission. TanDEM-X is implemented in the framework of a public-private partnership between the German Aerospace Center (DLR) and EADS Astrium GmbH. The TanDEM-X mission was successfully launched in June 2010 and started operational data acquisition in December 2010. This paper provides an overview of the TanDEM-X mission and summarizes its actual status and performance. Furthermore, results from several scientific radar experiments will be presented that show the great potential of future formation flying interferometric SAR missions to serve novel remote sensing applications.

I. INTRODUCTION

The primary objective of the TanDEM-X mission is the generation of a world-wide, consistent, timely, and high precision digital elevation model (DEM) as the basis for a wide range of scientific research, as well as for commercial DEM production ([1], cf. Figure 1). This goal is achieved by enhancing the TerraSAR-X synthetic aperture radar (SAR) mission [2] by a second radar satellite flying in close formation with TerraSAR-X [3]. Both satellites act together as a large single-pass SAR interferometer with the opportunity for flexible baseline selection. This enables the acquisition of highly accurate cross-track and along-track interferograms without the inherent accuracy limitations imposed by repeat-pass interferometry due to temporal decorrelation and atmospheric disturbances. Thanks to its unique capabilities, TanDEM-X will not only acquire a global DEM with unprecedented accuracy, but it will also be used to demonstrate numerous novel bistatic and multistatic SAR techniques and Earth observation applications that may form the basis for future formation flying SAR missions. TanDEM-X has been implemented in the framework of a public-private partnership between the German Aerospace Center (DLR) and EADS Astrium GmbH, as for TerraSAR-X.

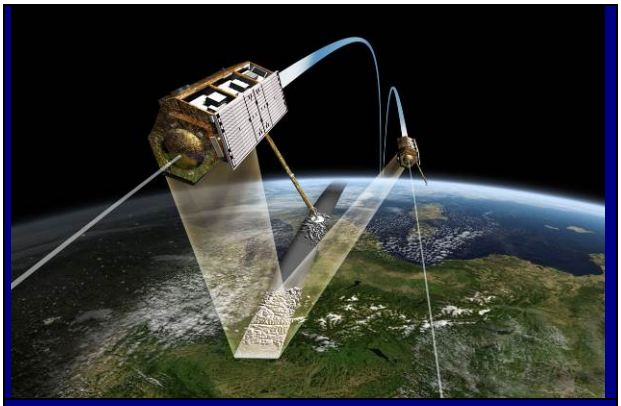

Acquisition of Global Digital Elevation Model

Parameter	Specification	Requirement
Relative Vertical Accuracy	90% linear point-to-point error in 1° cell	2 m (slope < 20%) 4 m (slope > 20%)
Absolute Vertical Accuracy	90% linear error	10 m
Spatial Resolution	independent pixels	12 m (0.4 arc sec)

Fig. 1: Primary objective of the twin-satellite mission TanDEM-X is the acquisition of a global Digital Elevation Model (DEM) with unprecedented accuracy.

II. MISSION CONCEPT

The TanDEM-X mission is an extension of the TerraSAR-X radar mission, co-flying a second satellite of nearly identical capability in a close formation. The TerraSAR-X satellite (TSX), as basis for TanDEM-X, was successfully launched into a sun-synchronous dusk-dawn orbit with 97.44° inclination on June 15, 2007. The nominal orbit height is 514.8 km and the orbit repeat cycle is 11 days. TSX is not only a high performance SAR system, but it has already built in all necessary features required for the implementation of the TanDEM-X mission. Examples are additional X-band horn antennas for inter-satellite phase synchronization, the availability of a dual-frequency GPS receiver for precise orbit determination, excellent RF phase stability of the SAR instrument, and PRF synchronization based on GPS as a common time reference. The second satellite (TDX) is as much as possible a rebuild of TSX with only minor modifications like an additional cold gas propulsion system for formation fine tuning and an additional S-band receiver to enable the reception of status and GPS position information broadcast by TSX. This similarity guaranteed a low development risk and offers the possibility for a flexible share of operational functions among the two satellites.

The instruments on both satellites are advanced high resolution X-band synthetic aperture radars based on active phased array technology, which can be operated in Spotlight, Stripmap, and ScanSAR mode with full polarization capability [4]. The center frequency of the instruments is 9.65 GHz with a selectable SAR chirp bandwidth of up to 300 MHz. The active phased array antenna, which has an overall aperture size of 4.8 m x 0.7 m, is fixed mounted to the spacecraft body and incorporates 12 panels with 32 dual-pol waveguide sub-arrays each. This enables agile beam pointing and flexible beam shaping as required for the acquisition of a wide range of image products with varying resolutions and scene sizes.

II.I Orbit Configuration and Formation Flying

The TanDEM-X operational scenario requires the coordinated operation of two satellites flying in close formation. The adjustment parameters for the formation are the orbits ascending nodes, the angle between the perigees, the orbit eccentricities and the phasing between the satellites. With these parameters, several options have been investigated during the phase A study, and the Helix satellite formation shown in Figure 2 has finally been selected for operational DEM generation. This formation combines an out-of-plane (horizontal) orbital displacement by different ascending nodes with a radial (vertical) separation by different eccentricity vectors resulting in a helix like relative movement of the satellites along the orbit. Since there exists no crossing of the satellite orbits, arbitrary shifts of the satellites along their orbits are allowed. This enables a safe spacecraft operation without the necessity for autonomous control. It is furthermore possible to optimize the along-track displacement at predefined latitudes for different applications: cross-track interferometry aims at along-track baselines which are as short as possible to ensure an optimum overlap of the Doppler spectra and to avoid temporal decorrelation in vegetated areas, while other applications like along-track interferometry or super resolution require selectable along-track baselines in the range from hundred meters up to several kilometres. A fine tuning of the satellite formation is performed via the aforementioned cold gas propulsion system on TDX.

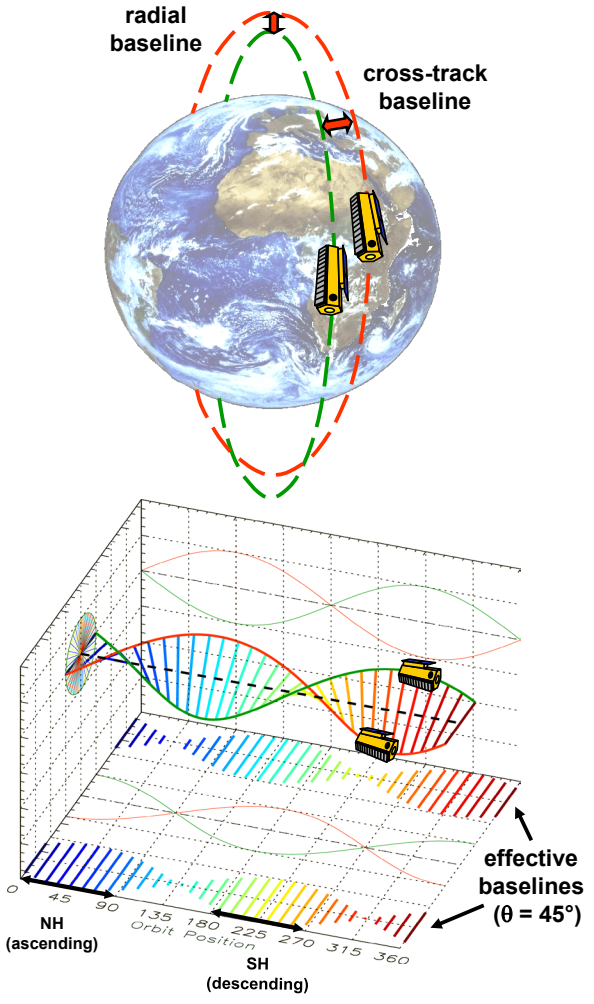

Fig. 2: Helix satellite formation for TanDEM-X. Top: illustration of orbits. Bottom: cross-track and radial baselines as a function of the argument of latitude. The latitude positions correspond to one complete orbit.

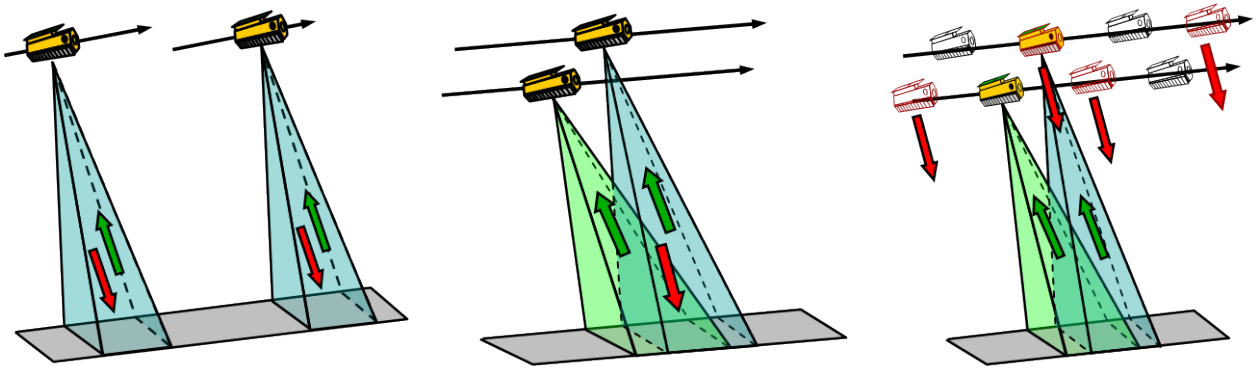

Fig. 3: Data acquisition configurations: Pursuit monostatic (left), bistatic (middle), and alternating bistatic (right).

The Helix formation enables a complete mapping of the Earth with a stable height of ambiguity by using a small number of formation settings [3]. Southern and northern latitudes can be mapped with the same formation by using ascending orbits for one and descending orbits for the other hemisphere, as illustrated in Figure 2 on the bottom. A fine tuning of the cross-track baselines can moreover be achieved by taking advantage of the natural rotation of the eccentricity vectors due to secular disturbances, also called motion of libration. The phases of this libration can be kept in a fixed relative position with small manoeuvres using the cold gas thrusters on a daily basis, while major formation changes as well as a duplication of the orbit keeping manoeuvres required by TSX will be performed by the hot gas thruster system.

II.II Interferometric Configurations and Modes

TanDEM-X can acquire interferometric data in different configurations: Examples are the Bistatic, Monostatic, and Alternating Bistatic modes as illustrated in Figure 3. The different interferometric configurations can be further combined with different TSX and TDX SAR imaging modes like Stripmap, ScanSAR, Spotlight, and Sliding Spotlight.

Operational DEM generation is planned to be performed using the bistatic Stripmap mode shown in Figure 3 in the middle. This mode uses either TSX or TDX as a transmitter to illuminate a common radar footprint on the Earth's surface. The scattered signal is then recorded by both satellites simultaneously. This simultaneous data acquisition makes dual use of the available transmit power and is mandatory to avoid possible errors from temporal decorrelation and atmospheric disturbances.

Another interferometric configuration is the pursuit monostatic mode which is illustrated in Figure 3 on the left. The two satellites are operated independently from each other in this mode, thereby avoiding the need for time and phase synchronization. The along-track distance between the satellites should be 20 km or more to avoid mutual RF interference between the two radar signals. This configuration has been used in the "monostatic commissioning phase" of TanDEM-X where several unique experiments have been conducted.

A third interferometric configuration is the alternating bistatic mode which is illustrated in Figure 3 on the right. The alternating bistatic mode is similar to the bistatic mode with the exception that the transmitter is switched from one satellite to the other on a pulse-to-pulse basis. This enables the simultaneous acquisition of multiple interferograms with two different effective baselines. Several experiments exploit this mode to get additional information, e.g., in vegetated areas.

II.III Exclusion Zones

For DEM generation, TanDEM-X combines one monostatic and one bistatic radar image in a joint SAR interferogram. To ensure a sufficient overlap of the Doppler spectra, this requires a short along-track distance of typically less than 1 km between the two satellites, while the radial and cross-track baselines depend on the argument of latitude and vary between zero and a few hundred meters. As a result, there is the danger that one satellite illuminates its partner by its radar antenna, which could cause interference, or, in the worst case, damage of sensitive electronic equipment. To avoid this risk, the transmission of radar signals has to be suppressed for one satellite at specific arguments of latitude, which are known as exclusion zones (cf. Figure 4). TanDEM-X ensures exclusion zone compliance by a double fail save approach including both a check on ground before command uploading and an additional real-time check on the satellite which suppresses signal transmission within predefined latitude windows.

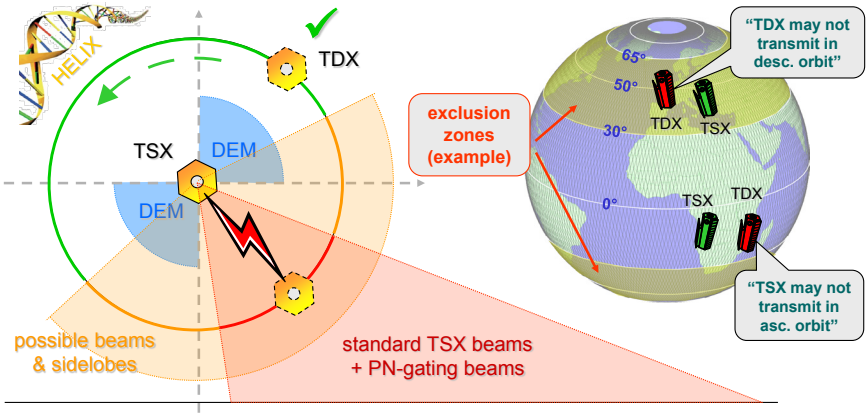

Fig. 4: TanDEM-X exclusion zones.

II.IV System Synchronization

A peculiarity of the bistatic data acquisition is the use of independent oscillators for the modulation and demodulation of the radar pulses. Any deviation between the two oscillators will hence cause a residual modulation of the recorded azimuth signal. The impact of oscillator phase noise in bistatic SAR has been analysed in [5] where it is shown that oscillator noise may cause significant errors in both the interferometric phase and SAR focusing. The stringent requirements for interferometric phase stability in the bistatic mode will hence require an appropriate relative phase referencing between the two SAR instruments or an operation in the alternating bistatic mode. For TanDEM-X, a dedicated inter-satellite X-band synchronization link has been established via mutual exchange of radar pulses between the two satellites. For this, the nominal bistatic SAR data acquisition is shortly interrupted, and a radar pulse is redirected from the main SAR antenna to one of six dedicated synchronization horn antennas mounted on each spacecraft. The pulse is then recorded by the other satellite which in turn transmits a short synchronization pulse (cf. Figure 5, top). By this, a bidirectional link between the two radar instruments is established, which allows for mutual phase referencing without exact knowledge of the actual distance between the satellites. On ground, a correction signal can then be derived from the recorded synchronization pulses. This compensates the oscillator induced phase errors in the bistatic SAR signal. The performance of such a synchronization link has been investigated in [6]. The bottom diagram in Figure 5 shows the predicted standard deviation of the residual phase errors after synchronization as a function of the update frequency of the synchronization signals for different signal-to-noise ratios (SNR) of the bidirectional link. The actual SNR varies with the distance between the satellites as well as their relative attitude. For the typical DEM data acquisition mode with baselines below 1 km, the SNR will be in the order of 30 to 40 dB, and it becomes clear that a phase error below 1° can be achieved for synchronization frequencies above 5 Hz.

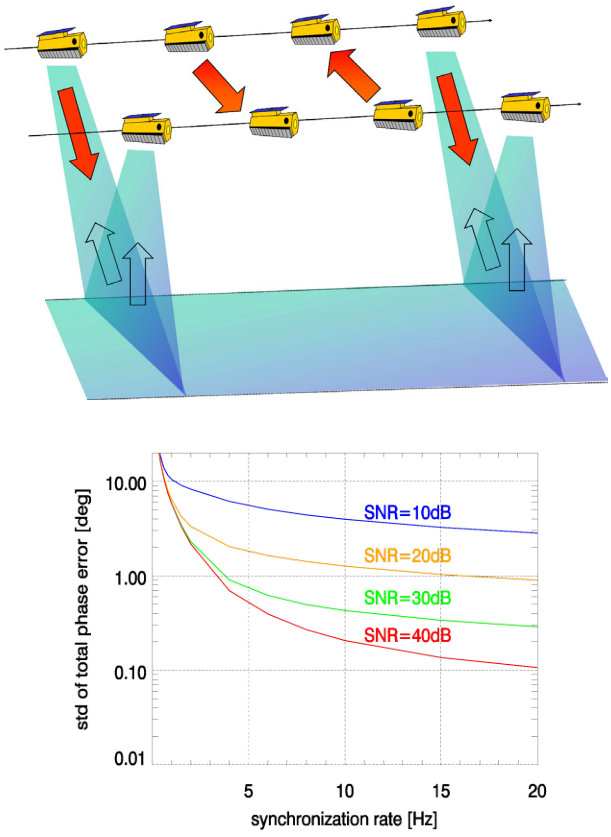

Fig. 5: Synchronization of TanDEM-X satellites by exchange or radar pulses (left) and predicted performance (right). The performance is shown in terms of the standard deviation of the total synchronization link phase error as a function of the synchronization frequency with signal-to-noise ratio as a parameter.

The performance of the synchronization link has been validated during the bistatic TanDEM-X commissioning phase [7]. Note that the correct application of the sync-link signal during bistatic SAR processing has to take into account relativistic effects since bistatic SAR processing and bistatic radar synchronization are performed in different reference frames moving relative to each other. This introduces a notable non-simultaneity between transmit and receive events which depends on the along-track distance between the two satellites [8]. The effect can be approximated based on Einstein's special relativity by comparing the corresponding spacetime intervals

$$s^2 = (c \cdot t_m)^2 - \left|\vec{B}_{Tx-Rx}\right|^2 = \left(c \cdot \frac{r_{bi}}{c}\right)^2 - \left|\vec{B}_{Tx-Rx} + \vec{v}_{Rx}\frac{r_{bi}}{c}\right|^2$$

$$\longrightarrow \quad r_{bi} \approx \vec{B}_{Tx-Rx}\frac{\vec{v}_{Rx}}{c} + c \cdot t_m$$

where s denotes the spacetime interval, c the velocity of light, t_m the radar pulse travelling time measured in the satellite reference frame, $\vec{B}_{Tx-Rx}$ the baseline vector connecting the master and slave satellites (length contraction can be neglected), r_{bi} the bistatic range, and $\vec{v}_{Rx}$ the velocity of the receiving satellite. The actual results with TanDEM-X show that this approximation provides a sufficient correction, even though it neglects the effect of Earth rotation which introduces an accelerated reference frame requiring a more rigorous treatment using, e.g., tensorial calculus of general relativity.

II.V Interferometric Performance and Global Data Acquisition Plan

Radar interferometry is based on the evaluation of the phase difference between two coherent radar signals acquired from slightly different spatial and/or temporal positions. By this, TanDEM-X is able to measure the range difference between the two satellites and a given scatterer with millimetric accuracy. The height of the scatterer is inferred from this range difference by geometric triangulation. The sensitivity of the phase-to-height scaling depends on the distance between the two satellites, where a larger baseline increases the sensitivity of the radar interferometer to small height variations. However, the conversion from phase to range and hence the conversion of phase differences to height is not unique, since the range difference measurement via phases is ambiguous with the wavelength. Radar interferometry expresses this ambiguity by the so called height of ambiguity.

$$h_{amb} = \frac{\lambda r_0 \sin(\theta_i)}{B_\perp}$$

where λ is the wavelength, r_0 the slant range from the satellites to the scatterer under consideration, θ_i the local incident angle of the electromagnetic wave, and $B_\perp$ is the perpendicular baseline. The scalar value $B_\perp$ is obtained by projecting the vector connecting both satellites onto a plane normal to the satellite orbit and then again onto a plane perpendicular to the line of sight.

Figure 6 shows the predicted height accuracy as a function of ground range position and the height of ambiguity (cf. [3] for details). It becomes clear that a lower height of ambiguity (i.e. larger baseline $B_\perp$) improves the height accuracy. However, a lower height of ambiguity also increases the difficulties in selecting the correct ambiguity interval during DEM generation (phase unwrapping). To minimize such problems and to ensure a homogeneous performance, TanDEM-X combines acquisitions with different heights of ambiguity. This requires in turn frequent adjustments of the Helix formation parameters which are selected according to an optimized global data acquisition plan [3]. Important constraints in this challenging optimization procedure are besides the interferometric performance the available amount of fuel and thruster cycles, limitations in the onboard storage and downlink capacity in combination with the finite time for global DEM acquisition, as well as power and thermal constraints. Further challenges arise from the interleaved usage of both satellites to continue the TerraSAR-X mission.

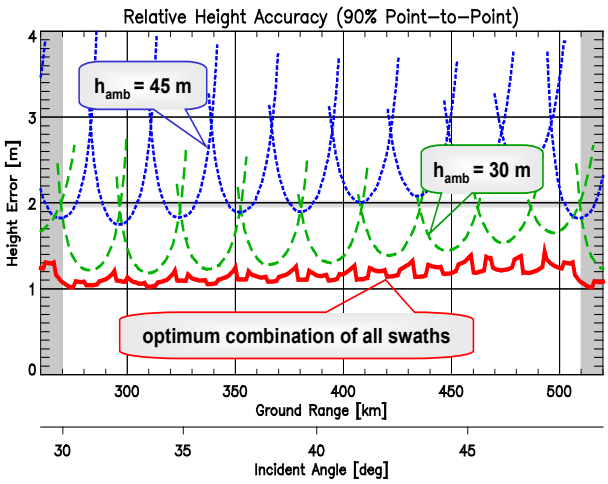

Fig. 6: Predicted height accuracy for a height of ambiguity of 45 m (dotted) and 30 m (dashed). The lower solid curve shows the error resulting from the combination of multiple swaths. All errors are point-to-point height errors for a 90% confidence interval. Systematic height accuracy evaluations of repeatedly acquired TanDEM-X DEMs show a good agreement with the performance model (cf. [9]).

II.VI Baseline Estimation and DEM Calibration

Up to now, we have neglected errors due to the finite accuracy of relative baseline estimation. Such errors will mainly cause a low frequency modulation of the DEM, thereby contributing simultaneously to relative and absolute height errors. Most critical for TanDEM-X are baseline errors in the line of sight ($\Delta B_{\parallel}$) which cause a rotation of the reconstructed DEM about the (master) satellite position. As a result, the DEM will be vertically displaced by

$$\Delta h = r \cdot \sin(\theta_i) \cdot \frac{\Delta B_{\parallel}}{B_{\perp}} = \frac{h_{amb}}{\lambda} \cdot \Delta B_{\parallel}$$

where r and θ_i are the slant range distance and the incident angle of an appropriately selected reference point (e.g. at mid swath). This vertical displacement will be $\Delta h = \pm 1.1$ m for $\Delta B_{\parallel} = \pm 1$ mm and $h_{amb} = 35$ m. A parallel baseline error will furthermore cause a tilt of the DEM which is given by

$$\varphi_{tilt} = \frac{\Delta h}{\Delta s} = \frac{\Delta B_{\parallel}}{B_{\perp}}$$

where Δs is the ground range distance from the selected reference point. The resulting tilt will be 3.8 mm/km and 2.3 mm/km for incident angles of $\theta_i = 30°$ and $\theta_i = 45°$, respectively ($\Delta B_{\parallel} = 1$ mm and $h_{amb} = 35$ m).

Precise baseline determination is performed by a double differential evaluation of GPS carrier phase measurements. The results from the TanDEM-X mission show that the relative satellite positions can be estimated with accuracies in the order of 1-2 mm. These results are also in good agreement with prior experience from the GRACE mission [10].

Additional systematic height error sources include uncompensated offsets from the SAR antenna phase centres, uncompensated internal delays in the SAR instruments, the use of different synchronization horn antennas for different orbit positions, the formation of the bistatic replica for both synchronization and bistatic imaging, as well as residual errors in the bistatic SAR processing, e.g. due to relativistic effects and Earth rotation (see also Section II.IV). A calibration for all these systematic phase offsets has been performed by evaluating the DEM height offset statistics over large data sets distributed all over the world [11]. By this, the typical height offsets of single DEM acquisitions are already well below the 10 m requirement from Figure 1 [12]. The final calibration of the global DEM is based on a bundle block adjustment using all overlapping TanDEM-X DEM data takes in combination with an appropriately selected subset of height references which are primarily obtained from the ICESat mission [13], [14]. From this, it may be expected that the absolute height accuracy of the globally mosaicked DEM will be significantly better than the required 10 m.

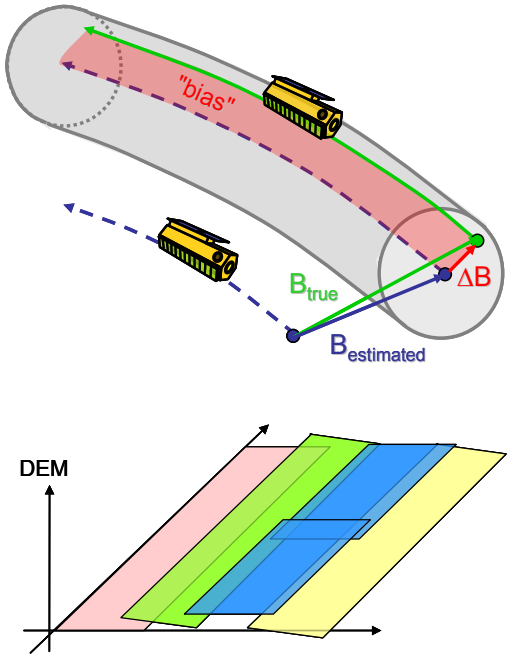

Fig. 7: Illustration of the impact of baseline estimation errors. Top: unknown baseline offset during each data take. The baseline measurement accuracy of 1-2 mm is indicated by the grey tube. Bottom: Vertical displacement and tilt of adjacent swaths as a result of different baseline offsets during the data takes.

III. STATUS SUMMARY

TanDEM-X was successfully launched on June 21, 2010. The initial separation between TDX and TSX was 15700 km and after one month of drifting a formation in pursuit monostatic configuration with an along-track distance of 20 km was reached [15]. This formation was maintained for 3 months to calibrate the TanDEM-X radar instruments and to perform first bistatic and interferometric experiments employing large baselines. On October 14, both satellites were maneuvered into a close formation to start the bistatic commissioning phase. During this phase, the radial and cross-track baselines were kept constant at 360 and 400 m, respectively, and the mean along-track distance was set to 0 m. The results from both the mono- and bistatic commissioning phase already demonstrated the unique interferometric performance of TanDEM-X [7].

Operational DEM acquisition started on December 12, 2010, less than 6 months after satellite launch. Since then, the total landmass of the Earth has been mapped once with a height of ambiguity ranging from 40 to 60 m. Global DEM data acquisition with varying baselines will continue until 2013, mapping difficult terrain like mountains, valleys, tall vegetation, etc., with at least two heights of ambiguity as well as from

multiple incidence/aspect angles. The latter will be achieved by swapping the Helix formation. This allows for a shift of the DEM acquisition quadrants from ascending to descending orbits in the northern hemisphere and vice versa in the southern hemisphere. The fully mosaicked DEM shall become available in 2014 for 90 % of the global landmass. Figure 8 shows two examples of TanDEM-X DEMs that have been acquired during the commissioning phase.

Ongoing work includes continuous performance monitoring and verification [16], [17], [18], [19], the acquisition for the remaining DEM data takes with optimized imaging geometries [20], multibaseline interferometric processing [21], [22], the final implementation, test and validation of the mosaicking and calibration processor [23], as well as the planning and conduction of bistatic and multistatic radar experiments within the science service segment [24].

IV. TANDEM-X EXPERIMENTS

TanDEM-X provides the remote sensing scientific community not only with a global DEM of unprecedented accuracy, but also with a unique reconfigurable SAR system to demonstrate novel bistatic and multistatic radar techniques for enhanced bio- and geophysical parameter retrieval. The following subsections summarize some of the advanced capabilities of TanDEM-X which can be operated in a multitude of modes and configurations [3]. Most of the provided results were already obtained during the TanDEM-X commissioning phase. The main intention of this section is to give the reader a first impression of the manifold capabilities of future formation flying SAR missions to serve novel remote sensing applications. A complete description of the experiments and a detailed discussion of their results can be found in the provided references.

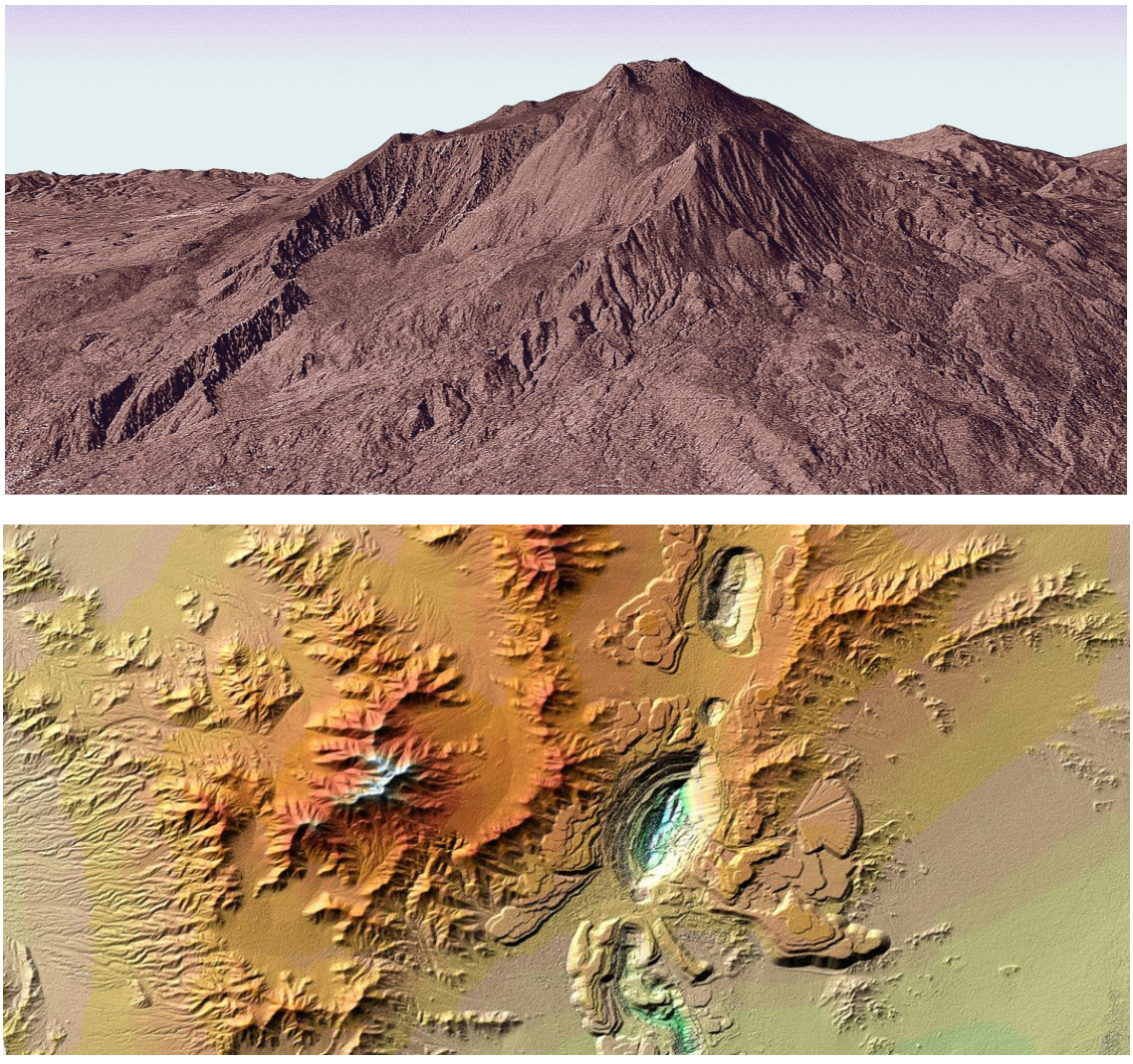

Fig. 8: Examples of digital elevation models acquired by TanDEM-X. Top: Italian volcano Mount Etna, located on the east coast of Sicily. Bottom: Chuquicamata, the biggest copper mine in the world, located in the north of Chile.

IV.I Velocity Measurements from Space

TanDEM-X has the capability to provide highly accurate velocity measurements of moving objects within a large coverage area. This can be achieved by comparing the amplitude and phase of two SAR images acquired at slightly different times (Figure 9). By adjusting the along-track displacement between the TDX and TSX satellites from almost zero to several tens of kilometres, TanDEM-X can adapt its sensitivity to a broad spectrum of velocities ranging from less than a millimetre per second to more than hundred kilometres per hour. The Helix satellite formation employed by TanDEM-X enables even a minimization of the effective across-track baseline for a given latitude and incident angle, thereby reducing the complexity in the velocity estimation process. Along-track interferometry can furthermore be enhanced by the so-called dual-receive antenna mode in each of the two tandem satellites, which provides additional phase centres separated by a short along-track baseline of 2.4 m. The combination of short and long baseline SAR data acquisitions improves both the detection and localization of moving objects and resolves phase ambiguities in case of fast scatterers. TanDEM-X provides hence a unique SAR system with four phase centres separated in the along-track direction. Potential applications are Ground Moving Target Indication (GMTI), the measurement of ocean currents, as well as the monitoring of sea ice drift and rotation.

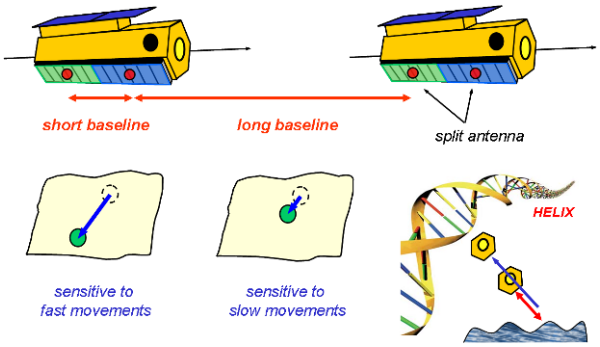

Fig. 9: Velocity measurements with TanDEM-X. The Helix satellite formation allows a flexible adjustment of the desired along-track separation between the satellites. In addition, a short along-track baseline is provided by each satellite.

Figure 10 shows as a first example the observation of ship movements in the Strait of Gibraltar [25]. The data were acquired during the monostatic commissioning phase where the satellites had an along-track separation of 20 km. This separation corresponds to a time lag of 2.6 seconds. The 2-D velocity vector could be measured with an accuracy of 1km/h by comparing the ship positions in the TSX and TDX SAR images (cf. [25] for details). The velocity measurements have been validated with independent data obtained from the Automatic Identification System (AIS).

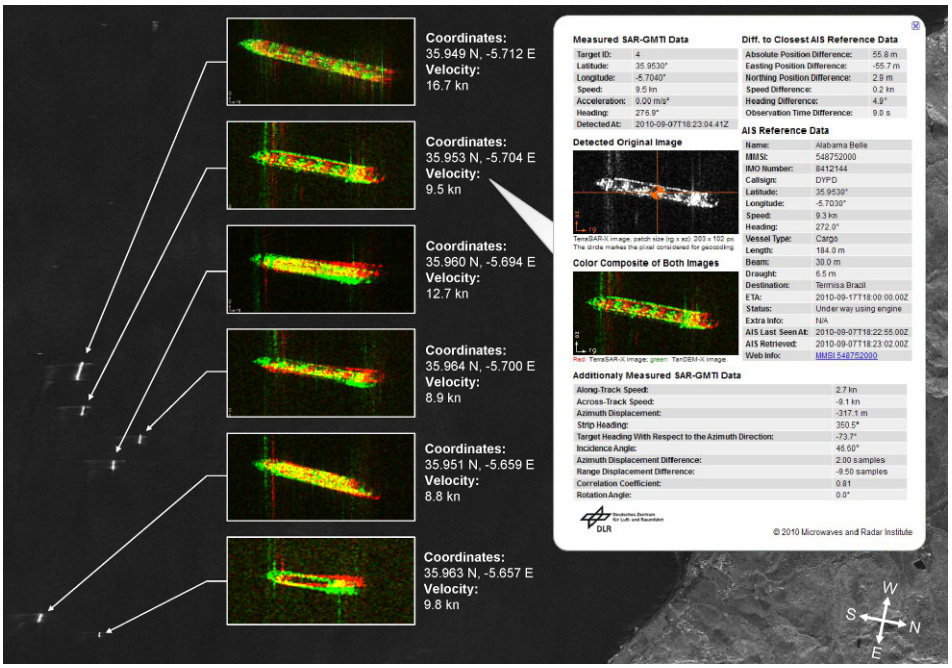

Fig. 10: Ship movements observed with TanDEM-X during the monostatic commissioning phase. The ship displacements can be seen from the insets showing TSX and TDX image patches overlaid in different colours. The estimated velocities are in excellent agreement with AIS reference data (right, cf. [25] for more details).

IV.II Large Baseline Cross-Track Interferometry

Large baseline interferometry takes advantage of the high RF bandwidth of the TSX and TDX satellites, allowing for coherent data acquisitions with cross-track baselines of up to 5 km and more. Note that less than 5% of the maximum possible (critical) baseline length is used during nominal DEM data acquisition. Large baseline interferograms can hence significantly improve the height accuracy beyond the standard TanDEM-X DEM quality, but the associated low height of ambiguity requires typically a combination of multiple interferograms with different baseline lengths to resolve phase ambiguities, especially in hilly and mountainous terrain. Further opportunities arise from a comparison of multiple large baseline TanDEM-X interferograms acquired during different passes of the satellite formation (Figure 11). This provides a sensitive measure for vertical scene and structure changes. Potential applications are a detection of the grounding line which separates the shelf from the inland ice in polar regions, monitoring of vegetation growth, mapping of atmospheric water vapour with high spatial resolution, measurement of snow accumulation or the detection of anthropogenic changes of the environment, e.g. due to deforestation. Note that most of these combinations rely on a comparison of two or more single-pass (large baseline) cross-track interferograms and do hence not necessarily require coherence between the different passes. Further information can be gained from an evaluation of coherence changes, potentially augmented by polarimetric information. This is for instance well suited to reveal even slight changes in the soil and vegetation structure reflecting vegetation growth and loss, freezing and thawing, fire destruction, human activities, and so on. The combination of repeated TanDEM-X single-pass interferograms enables hence the entry into a new era of interferometric and tomographic 3-D and 4-D SAR imaging as it was ERS-1/2 for the development of classical repeat-pass SAR interferometry.

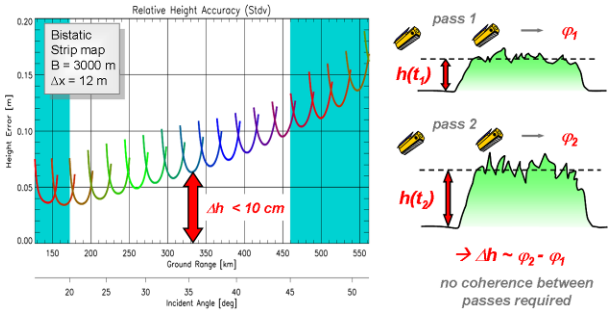

Fig. 11: Performance estimation for large baseline DEM acquisitions with TanDEM-X (cross-track baseline = 3000 m, posting = 12 m). A relative height accuracy (single point standard deviation) better than 10 cm is predicted.

Figure 12 shows as a first example a large baseline DEM which was acquired by TanDEM-X on July 16, 2010 in the Russian Arctic (October Revolution Island) [26]. The DEM was part of a longer data take that used a sophisticated commanding to obtain a large baseline interferogram while TDX was still drifting towards TSX from its initial along-track separation of 15700 km. At the time of data acquisition, the two satellites were 380 km apart from each other, resulting in a temporal separation of 50 seconds. Earth rotation caused a cross-track baseline of 2 km which corresponds to a height of ambiguity of only 3.8 m. A squinted operation was necessary to provide a sufficient overlap of the Doppler spectra. The right hand side of Figure 4 shows the predicted (black curve) and estimated (gray curve) standard deviation of the point-to-point relative height error for a linear slice through the DEM. The predicted error was calculated from the coherence measurements and the estimated error was obtained by high-pass filtering the DEM slice [26]. Both results show that the height accuracy is in the order of 20 cm. This demonstrates the great potential of formation flying SAR missions to obtain high resolution elevation information with decimeter accuracy, thereby enabling new remote sensing applications. An example is the monitoring of height changes over glaciers, ice caps or ice sheets to quantify their ice mass balance and a dedicated formation flying SAR mission has already been proposed for this purpose [27].

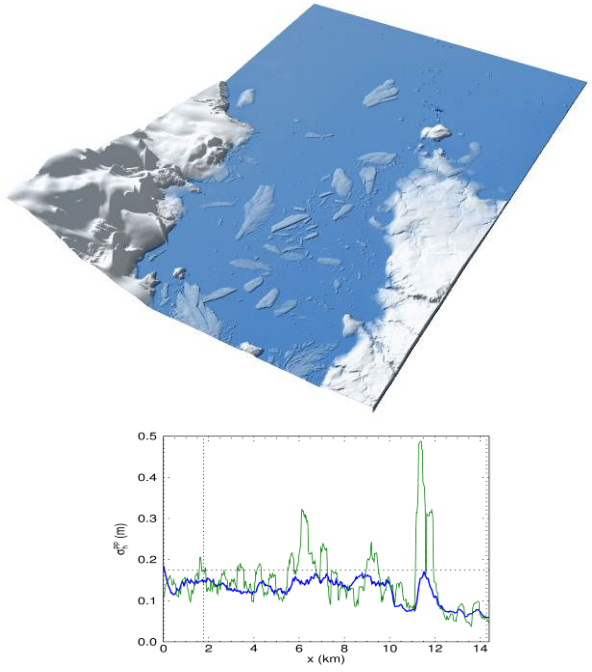

Fig. 12: Large baseline TanDEM-X DEM from the border of October Revolution island (left) and predicted (black) vs. estimated (gray) point-to-point height accuracy along a DEM slice (cf. [26] for details).

IV.III Polarimetric SAR Interferometry

Polarimetric SAR interferometry combines interferometric with polarimetric measurements to gain 3-D structure information from semi-transparent volume scatterers in a single pass [28]. A prominent example is the measurement of vegetation height and density which forms also the basis of future formation flying SAR missions dedicated to global environmental monitoring. Figure 13 shows as an example the height differences obtained for a dual-polarized TanDEM-X spotlight acquisition of an agricultural field in Russia. The data were acquired during the monostatic commissioning phase with a perpendicular baseline of 275 m, demonstrating the potential of crop height estimation. Current and future experiments will also combine multiple interferometric data takes acquired in dual and fully polarimetric modes [29], [30].

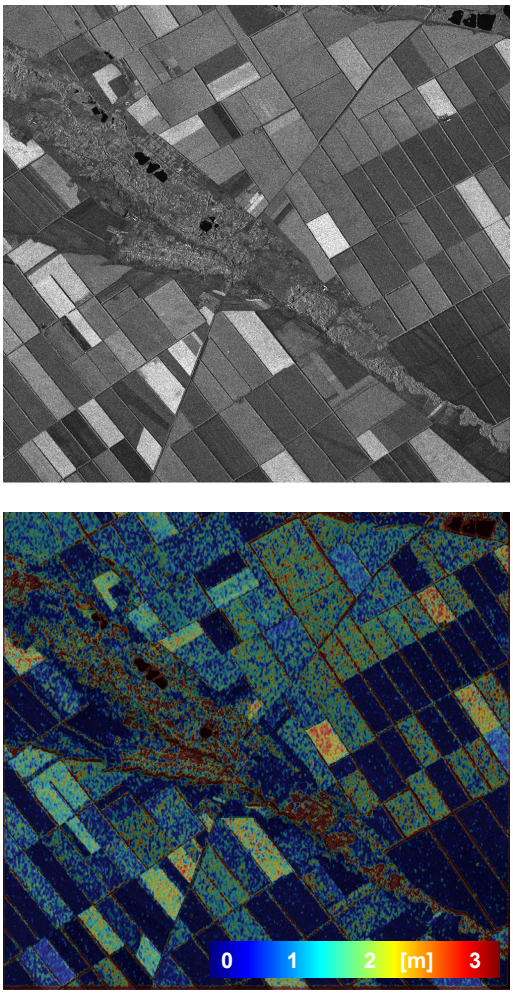

Fig. 13: Polarimetric SAR interferometry with TanDEM-X. Top: amplitude of SAR image. Bottom: interferometric height difference between HH and VV channels.

IV.IV Bistatic SAR Imaging

Polarimetric Bistatic SAR imaging provides additional observables for the extraction of important scene and target parameters. TanDEM-X allows for the simultaneous acquisition of bistatic and monostatic images in a single data take to obtain a highly informative set of multi-angle observations. A quantitative evaluation of the bistatic radar cross-section (RCS) and a comparison with its monostatic equivalent facilitates the detection and recognition of targets. The segmentation and classification in radar images is expected to be improved by comparing the spatial statistics of mono- and bistatic scattering coefficients. This is supported by airborne bistatic radar experiments performed by DLR and ONERA, which revealed significant changes of the scattering behaviour for both artificial and natural targets even in case of rather small bistatic angles. A joint evaluation of mono- and bistatic SAR images could also be used to isolate different scattering mechanisms. An example is the distinction between highly directive dihedral returns from more isotropic volume scattering. Bistatic SAR has moreover potential for the retrieval of sea state parameters, the estimation of surface roughness and terrain slope, as well as stereogrammetric, meteorological and atmospheric applications. The bistatic data acquired with TanDEM-X will hence provide a unique data source to improve our understanding of bistatic SAR imaging and its exploitation for future remote sensing applications. A first bistatic data take has been acquired over Brasilia during the monostatic commissioning phase where the satellites were separated by 20 kilometers. Figure 14 shows an overlay of the bistatic SAR image with its monostatic counterpart demonstrating significant scattering differences already for very small bistatic angles [31].

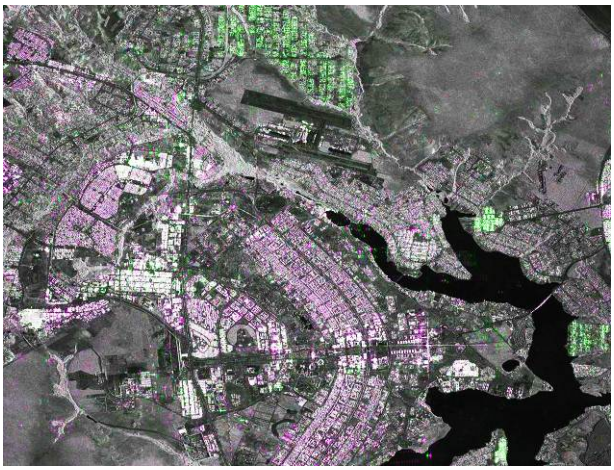

Fig. 14: Overlay of monostatic (magenta) and bistatic (green) SAR image.

V. CONCLUSIONS

The TanDEM-X mission opens a new era in spaceborne radar remote sensing. A large single-pass SAR interferometer with adjustable baselines has been formed by adding a second, almost identical radar satellite to TerraSAR-X and flying both satellites in a closely controlled formation. This enables not only the acquisition of a global DEM with unprecedented accuracy, but also the demonstration of highly innovative bistatic and multistatic SAR techniques and applications. These experiments form the basis for future formation flying SAR missions [32].

Key technologies like close formation flying, bistatic SAR operation and synchronisation, precise baseline estimation and calibration as well as sophisticated bistatic and interferometric processing chains have been implemented. Appropriate safety mechanisms allow for safe operation at typical satellite distances between 150 m and 1000 m. The complete mission is fully operational since December 2010 and both satellites as well as the ground system perform remarkably well. Current fuel consumption and battery degradation on the TerraSAR-X satellite is well below specification and will probably allow for life time extensions of two to three years, i.e. close formation flying until 2015 seems feasible. The prolonged mission time will allow for additional DEM acquisitions with improved accuracy and resolution as well as the conduction of advanced bistatic and multistatic SAR experiments in unique configurations, modes and geometries.

ACKNOWLEDGMENT

We highly acknowledge the great effort and enthusiasm of all our colleagues at DLR and EADS Astrium who made this ambitious mission a reality. TanDEM-X is partly funded by the German Federal Ministry for Economics and Technology (50 EE 0601) and realized in a public-private partnership between German Aerospace Center (DLR) and Astrium GmbH.

REFERENCES

[1] A. Moreira, G. Krieger, I. Hajnsek, M. Werner, D. Hounam, S. Riegger, E. Settelmeyer, “TanDEM-X: A TerraSAR-X Add-On Satellite for Single-Pass SAR Interferometry,” in Proc. IGARSS, Anchorage, USA, 2004.

[2] R. Werninghaus and S. Buckreuss, “The TerraSAR-X Mission and System Design,” IEEE Transactions on Geoscience and Remote Sensing, vol. 48, no. 2, pp. 606–614, Feb. 2010.

[3] G. Krieger, A. Moreira, H. Fiedler, I. Hajnsek, M. Werner, M. Younis, M. Zink, “TanDEM-X: A Satellite Formation for High Resolution SAR Interferometry,” IEEE Transactions on Geoscience and Remote Sensing, vol. 45, no. 11, pp. 3317-3341, 2007.

[4] W. Pitz and D. Miller, “The TerraSAR-X Satellite” IEEE Transactions on Geoscience and Remote Sensing, vol. 48, no. 2, pp. 615–622, Feb. 2010.

[5] G. Krieger and M. Younis, “Impact of Oscillator Noise in Bistatic and Multistatic SAR,” IEEE Geoscience and Remote Sensing Letters, vol. 3, pp. 424- 428, 2006.

[6] M. Younis, R. Metzig, G. Krieger, “Performance Prediction of a Phase Synchronization Link for Bistatic SAR,” IEEE Geoscience and Remote Sensing Letters, vol. 3, pp. 429- 433, 2006.

[7] http://www.dlr.de/Portaldata/32/Resources/dokumente/tdmx/sciencemeeting3/08-Interferometric_Performance_Handout_small.pdf

[8] G. Krieger and F. de Zan, “Relativistic Effects in Bistatic SAR Processing and System Synchronization,” European Conference on Synthetic Aperture Radar (EUSAR), Nuremberg, Germany, April 2012.

[9] P. Rizzoli, B. Bräutigam, T. Kraus, M. Martone, G. Krieger, “Relative height error analysis of TanDEM-X elevation data,” ISPRS Journal of Photogrammetry and Remote Sensing, 2012.

[10] M. Wermuth, O. Montenbruck, A. Wendleder, “Relative Navigation for the TanDEM-X Mission and Evaluation with DEM Calibration Results”, 22nd International Symposium on Spaceflight Dynamics; 28 Feb. - 4 March 2011, Sao Jose dos Campos, Brazil (2011).

[11] J. Hueso González, J. Walter Antony, M. Bachmann, G. Krieger, M. Zink, D. Schrank, M. Schwerdt, “Bistatic system and baseline calibration in TanDEM-X to ensure the global digital elevation model quality,” ISPRS Journal of Photogrammetry and Remote Sensing, 2012.

[12] M. Bachmann, J. Hueso Gonzalez, G. Krieger, M. Schwerdt, J. Walter Antony, F. De Zan, “Calibration of the Bistatic TanDEM-X Interferometer,” European Conference on Synthetic Aperture Radar (EUSAR), Nuremberg, Germany, April 2012.

[13] J. Hueso Gonzalez, M. Bachmann, G. Krieger, H. Fiedler, “Development of the TanDEM-X Calibration Concept: Analysis of Systematic Errors”, IEEE Trans. Geosci. Remote Sens., vol. 48, no. 2, pp. 716–726, Feb. 2010.

[14] A. Gruber, B. Wessel, M. Huber, A. Roth, "Operational TanDEM-X DEM calibration and first validation results," ISPRS Journal of Photogrammetry and Remote Sensing, 2012.

[15] R. Kahle, B. Schlepp, F. Meissner, M. Kirschner, R. Kiehling, "TerraSAR-X / TanDEM-X Formation Acquisition – Analysis and Flight Results", 21st AAS/AIAA Space Flight Mechanics Meeting, 13-17 Feb. 2011, New Orleans, Louisiana.

[16] M. Martone, B. Bräutigam, P. Rizzoli, C. Gonzalez, M. Bachmann, G. Krieger, "Coherence Evaluation of TanDEM-X Interferometric Data," ISPRS Journal of Photogrammetry and Remote Sensing, 2012.

[17] B. Bräutigam, P. Rizzoli, M. Martone, M. Bachmann, T. Kraus, G. Krieger, "InSAR and DEM Quality Monitoring of TanDEM-X," International Geoscience and Remote Sensing Symposium (IGARSS), Munich, Germany, July 2012.

[18] M. Villano, G. Krieger, "Impact of Azimuth Ambiguities on Interferometric Performance," IEEE Geoscience and Remote Sensing Letters, vol. 9, no. 5, pp. 896-900, 2012.

[19] F. De Zan, G. Krieger, P. Lopez Dekker, "On Some Spectral Properties of TanDEM-X Interferograms Over Forested Areas," IEEE Geoscience and Remote Sensing Letters, vol. 10, no. 1, pp. 71-75, 2013.

[20] M. Bachmann, D. Schulze, C. Ortega Miguez, D. Polimeni, J. Böer, J. Hueso Gonzalez, J. Walter Antony, G. Krieger, B. Bräutigam, M. Schwerdt, M. Zink, "TanDEM-X Acquisition Status and Calibration of the Interferometric System," International Geoscience and Remote Sensing Symposium (IGARSS), Munich, Germany, July 2012.

[21] T. Fritz, H. Breit, C. Rossi, U. Balss, M. Lachaise, U. Duque, "Interferometric Processing and Products of the TanDEM-X Mission", International Geoscience and Remote Sensing Symposium (IGARSS), Munich, Germany, July 2012.

[22] M. Lachaise, U. Balss, T. Fritz, H. Breit, "The Dual-Baseline Interferometric Processing Chain for the TanDEM-X Mission", International Geoscience and Remote Sensing Symposium (IGARSS), Munich, Germany, July 2012.

[23] A. Gruber, B. Wessel, M. Huber, M. Breunig, S. Wagenbrenner, A. Roth, "Quality Assessment of First Larger TanDEM-X DEM Blocks," International Geoscience and Remote Sensing Symposium (IGARSS), Munich, Germany, July 2012.

[24] I. Hajnsek, T. Busche, "TanDEM-X: Science Activities," International Geoscience and Remote Sensing Symposium (IGARSS), Munich, Germany, July 2012.

[25] S. Baumgartner and G. Krieger, "Large Along-Track Baseline SAR-GMTI: First Results with the TerraSAR-X/TanDEM-X Satellite Constellation, in Proc. IGARSS, Vancouver, Canada, 2011.

[26] P. Lopez-Dekker, P. Prats, F. De Zan, D. Schulze, G. Krieger, A. Moreira, "TanDEM-X First DEM Acquisition: A Crossing Orbit Experiment", to appear in IEEE Geoscience and Remote Sensing Letters, 2011.

[27] T. Börner, F. de Zan, P. López-Dekker, G. Krieger, I. Hajnsek, K. Papathanassiou, M. Villano, M. Younis, A. Danklmayer, W. Dierking, T. Nagler, H. Rott, S. Lehner, T. Fügen, A. Moreira, "SIGNAL: SAR for Ice, Glacier and Global Dynamics", International Geoscience and Remote Sensing Symposium (IGARSS), Honolulu, Hawaii, July 2010.

[28] S.R. Cloude, K.P. Papathanassiou, "Polarimetric SAR interferometry," IEEE Transactions on Geoscience and Remote Sensing, vol. 36, pp. 1551-1565, 1998.

[29] F. Kugler, I. Hajnsek, K. Papathanassiou, "Dual Pol-InSAR Forest Height Estimation by Means of TanDEM-X Data," International Geoscience and Remote Sensing Symposium (IGARSS), Munich, Germany, July 2012.

[30] K. Papathanassiou, F. Kugler, I. Hajnsek, "Exploring the Potential of Pol-InSAR Techniques at X-band: Results and Experiments from TanDEM-X," International Geoscience and Remote Sensing Symposium (IGARSS), Munich, Germany, July 2012.

[31] M. Rodriguez-Cassola, P. Prats, D. Schulze, N. Tous-Ramon, U. Steinbrecher, L. Marotti, M. Nannini, M. Younis, P. Lopez-Dekker, M. Zink, A. Reigber, G. Krieger, and A. Moreira, First Bistatic Spaceborne SAR Experiments with TanDEM-X, IEEE Geoscience and Remote Sensing Letters, vol. 9, no. 1, pp. 33-37, 2012.

[32] G. Krieger, I. Hajnsek, K. Papathanassiou, M. Younis, A. Moreira, "Interferometric Synthetic Aperture Radar (SAR) Missions Employing Formation Flying", Proceedings of the IEEE, vol. 58, no. 5, pp. 816-843, 2010.